Numerical results of falling film absorption with water/ammonia [1]

Reindert H. Wassenaar [a], Guus Segal [b]*

[a] *Netherlands Energy Research Foundation ECN, P.O. Box 1, 1755 ZG Petten, The Netherlands*
[b] *Faculty of Information Technology and Systems, Delft University of Technology, P.O. Box 5031, 2600 GA Delft, The Netherlands*

Abstract — A model was set up for the heat, mass and momentum transport in a falling film absorber with a binary gas phase. Results are given for water/ammonia and countercurrent gas flow. If the ratio of diffusion to convection is not negligible (here for a gas channel smaller than 5 mm) absorption is higher with countercurrent gas flow than with cocurrent flow. For larger gas channels the outcomes from a simpler one-component gas phase model are, if the interface boundary conditions are formulated correctly, almost equal to the outcomes from the present model. © 1999 Éditions scientifiques et médicales Elsevier SAS

absorption / water–ammonia / film falling / modeling / heat and mass transfer

Nomenclature

A, B	constants in linearized interface thermodynamic equilibrium relation	K
a, D	heat, mass diffusivity	$m^2 \cdot s^{-1}$
h	enthalpy	$J \cdot kg^{-1}$
l	characteristic length	m
p	pressure	Pa
T	temperature	K
u, v	velocity component in x-, y-direction	$m \cdot s^{-1}$
w	mass fraction of ammonia in the mixture	$kg \cdot kg^{-1}$
x, y	co-ordinate along, perpendicular to the wall	m
α	heat transfer coefficient	$W \cdot m^{-2} \cdot K^{-1}$
Γ	flow rate per wetted unit of width . .	m^3 or $kg \cdot m^{-1} \cdot s^{-1}$
δ	film thickness	m
λ	heat conductivity	$W \cdot m^{-1} \cdot K^{-1}$
ρ	mass density	$kg \cdot m^{-3}$

Subscripts and superscripts

$'$	simple model

e	equilibrium
m	mass
0	entrance
f	fluid
x	in x-direction
c	cooling medium
g	gas
y	in y-direction

---

* Correspondence and reprints.
a.segal@twi.tudelft.nl

[1] This article is a follow up to a communication presented by the authors at the EUROTHERM 59 Conference, held in Nancy (France) in July 1998.

1. INTRODUCTION

Two mixtures are generally applied in absorption heat pumps: $LiBr/H_2O$ and H_2O/NH_3. In the past twenty years models for mixtures like $LiBr/H_2O$ have reached a high degree of sophistication. The pioneers started with analytical solutions for limiting cases [1], later numerical solutions were obtained for a flat laminar film along an isothermal wall [2]. Further progress was made by the addition of the counterflow, cocurrent or cross-flow cooled wall and two-dimensional film flow [3]. Interest in H_2O/NH_3 is increasing because with this mixture an absorber can be several times more compact than with $LiBr/H_2O$. Determining for the size of an absorber is the ratio D/a [3], for heat pump conditions

this ratio is about five times larger for H_2O/NH_3 than for $LiBr/H_2O$. Despite of this advantage, the relevant literature for H_2O/NH_3 is scarce. Several transfer coefficient models exist [4], and numerical solutions for related problems [5]. However, in [5] the second component in the gas phase is stagnant and the interfacial coupling between temperature and mass fraction is not taken into account. The model that is briefly outlined here ([6] gives an elaborate version) builds further on a model with a one-component gas phase [3] (called simple model in this paper), by adding the second component, and solving the transfer equations in the gas phase with a finite element method.

2. MODEL

2.1. Physical model

The model presented in this section is valid for a binary mixture with the same two components present in the vapour phase. The model applies to any mixture, but as an example the mixture water/ammonia is considered. *Figure 1* gives the geometry of the cooled falling film absorber. The model allows the cooling medium as well as the gas to flow in the same direction as the film, in the opposite direction, or in a direction perpendicular to the paper. The model of this absorber is built on the following assumptions:

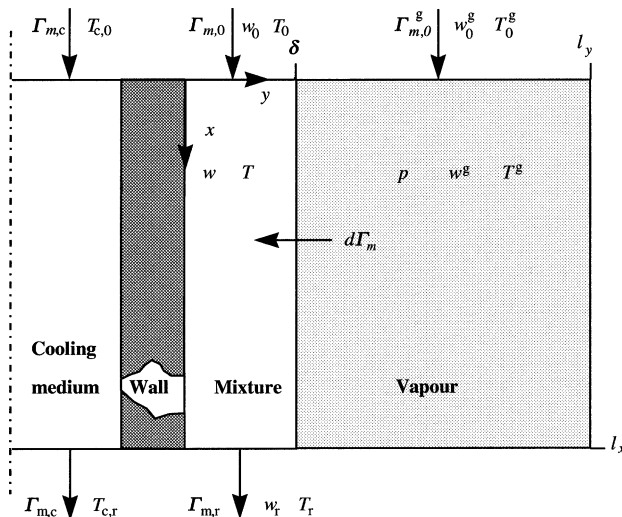(1) the absorber is in steady state and the gas flow is two-dimensional;

(2) the properties of cooling medium, liquid and vapour are constant, with a value based on the entrance conditions;

(3) the only forces acting on the film (the liquid is Newtonian) are gravity and wall friction;

(4) the change in mixture mass flow because of the absorption is negligible;

(5) at the interface vapour and liquid are in thermodynamic equilibrium, the relation between temperature and mass fraction is linear with constant coefficients (dashed lines in *figure 2*);

(6) all heat of absorption is released at the interface;

(7) the liquid is binary, in both phases the same components are present;

(8) heat in liquid and vapour phase is only transported by convection and conduction;

(9) mass in both phases is only transported by convection and (Fickian) diffusion;

(10) in the film transport of heat and mass along the wall is only by convection; transport perpendicular to the wall is only by heat or mass diffusion.
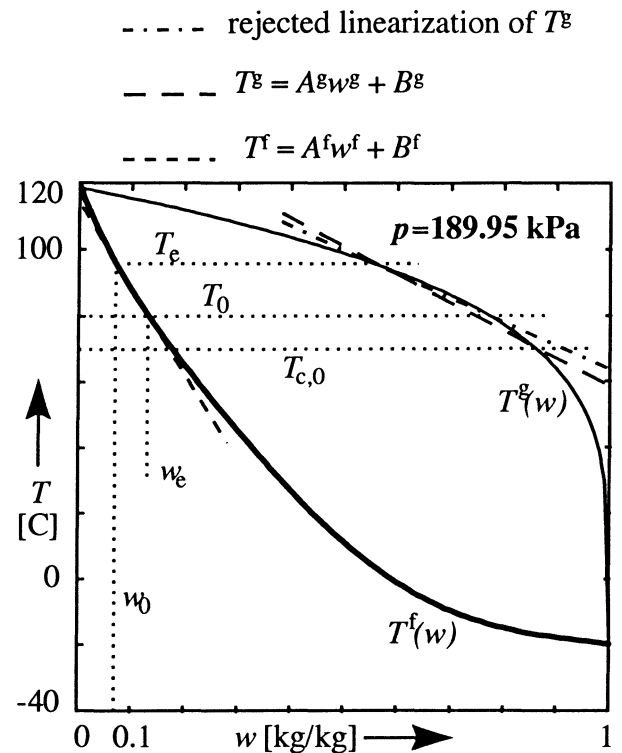

Figure 1. Geometry of a cooled falling film with a binary gas flow.

Figure 2. Equilibrium temperatures of the two-phase binary system water/ammonia at a pressure of 189.95 kPa. The bold line applies to the liquid, the other curve to the vapour.

Assumption (4) has to be made in order to simplify the liquid phase to a simple flat film, a logical result from this is that convection perpendicular to the wall is absent in the film. However, this does not mean that convection towards the wall is neglected: in Section 2.2 we will see that these terms are accounted for in the boundary conditions (2b) and (3d) at the interface.

Figure 2 gives the vapour and liquid equilibrium lines. The liquid curve is linearized between T_e (mass fraction w_0) and entrance temperature T_0 (mass fraction w_e). The vapour curve is linearized between T_e and the cooling medium entrance temperature $T_{c,0}$. The interface mass fraction at the absorber entry will have a value (depending on heat of absorption, and diffusivity) between w_0 and w_e. As a result, ammonia is absorbed from the vapour phase and transported into the film. The figure shows that the vapour equilibrium mass fraction is between 0.6 and 0.9 kg·kg^{-1}, resulting in a large water flow from the interface into the vapour phase.

2.2. Mathematical model

Heat transport is described by the convection–diffusion equation:

$$u^g \frac{\partial T^g}{\partial x} + v^g \frac{\partial T^g}{\partial y} = a^g \left(\frac{\partial^2 T^g}{\partial x^2} + \frac{\partial^2 T^g}{\partial y^2} \right) \qquad (1)$$

Mass transport is described by an equation of the same form, with w instead of T, and D instead of a. In the film the second left-hand term and the first right-hand term are absent. Vapour flow is described by the two-dimensional conservation equations of mass and momentum (Navier–Stokes). The film flow is described by the Nusselt solution (half-parabolic velocity profile). The vapour flow boundary conditions are: zero flow at the solid wall and a uniform entrance velocity. At the interface ($0 \leq x \leq l_x, \ y = \delta$) a continuity equation is valid:

$$u^g = u^f(\delta) \qquad (2a)$$

$$\rho^g v^g = \frac{-\rho^f D^f}{w^g - w^f} \frac{\partial w^f}{\partial y} + \frac{\rho^g D^g}{w^g - w^f} \frac{\partial w^g}{\partial y} \qquad (2b)$$

that couples the mass transfer equations to the velocity equations. The heat and mass transfer boundary conditions are: no transfer at the vapour walls, a cooling condition at the film wall, uniform entrance conditions, and at the interface:

$$T^f = A^f w^f + B^f \qquad (3a)$$

$$T^g = T^f \qquad (3b)$$

$$T^g = A^g w^g + B^g \qquad (3c)$$

$$-\lambda^f \frac{dT^f}{dy} + \lambda^g \frac{dT^g}{dy} = \frac{-\rho^f D^f}{w^g - w^f} \frac{dw^f}{dy} \Delta h^f$$
$$+ \frac{-\rho^g D^g}{w^g - w^f} \frac{dw^g}{dy} \Delta h^g \qquad (3d)$$

with A and B the coefficients that linearize the equilibrium relation at constant pressure (see *figure 2*), and Δh the heat of absorption defined by $\Delta h^f = h^g - h^f - (w^g - w^f)\partial h^f/\partial w$ and $\Delta h^g = h^g - h^f - (w^g - w^f)\partial h^g/\partial w$. Relations (2b) and (3d) result from the continuity of mass and heat transport at the interface. In a co-ordinate frame fixed to the wall, the local ammonia mass flow (per unit width) at the liquid side equals:

$$d\Gamma_{m,1}^f = -\rho^f D^f \frac{dw^f}{dy} dx + w^f d\Gamma_m \qquad (4)$$

The right-hand side of this equation not only contains a diffusion term, but also a convection term, the so-called drift term. Equating this mass flow to a similar expression for the gas side flow leads to the right-hand side of (2b). Combination with similar relations for the heat flow leads to equation (3d). For a one-component gas phase ($\partial w^g/\partial y = 0, \ w^g = 1$) equation (3d) shrinks to:

$$-\lambda^f \frac{dT^f}{dy} = \frac{-\rho^f D^f}{1 - w^f} \frac{dw^f}{dy} \Delta h^f \quad \text{with}$$

$$\Delta h^f = h^g - h^f - \left(1 - w^f\right) \frac{\partial h^f}{\partial w} \qquad (5)$$

Although the derivation of equation (3d) or the approximation (5) is straightforward [3, p. 62], there is no consensus of opinion in the literature on this approach. For example, reference [3] does neither take the drift term into account nor uses the partial enthalpy in Δh.

2.3. Finite element implementation

The mathematical model is implemented in a finite element formulation, the applied software is Sepran [7]. The boundary conditions (3) are non-standard, so the Sepran program had to be extended by one of the authors of the program, A. Segal. The flow equations and the heat and mass transfer equations are solved separately. From a start solution (one-component gas phase approximation) the boundary conditions for the interface velocity (2b)

Figure 3. The velocity vector in the mesh points in the gas phase for countercurrent gas flow.

can be calculated. Then a solution is calculated for the gas flow field. With these velocities, and the Nusselt velocities in the film, the convection–diffusion equations in both phases can be solved, resulting in updated interface velocity values. The accuracy of the outcomes is better than 1 %. The computer time on a 100 MHz 80486 (32-bit code) is approximately a quarter of an hour. For cross-flow and cocurrent gas flow smooth contour lines for temperature and mass fraction lines in the gas phase were found. For countercurrent gas flow this is not the case. Still several tests show that the overall outcomes, like Δw, are correct. Smooth lines can be obtained with up-winding, but this is not yet implemented in Sepran for the applied standard element.

3. RESULTS

3.1. Countercurrent gas flow results

The results presented here are derived for a vertical plate absorber with a length of 1 m, and a channel width of 5 mm. In *figures 3–5* the geometry of *figure 1* is rotated 90° counter clockwise. The entrance conditions are (superscript 'f' for the film is omitted):

$$T_0 = 80\,°\text{C} \qquad T_0^{\text{g}} = -20\,°\text{C}$$

$$w_0 = 0.07\,\text{kg·kg}^{-1} \qquad w_0^{\text{g}} = 1.00\,\text{kg·kg}^{-1}$$

$$p = 189.95\,\text{kPa} \qquad T_{\text{c},0} = 70\,°\text{C}$$

$$\Gamma = 89.275 \cdot 10^{-6}\,\text{m}^2\text{·s}^{-1}$$

$$\Gamma_c: \text{cross-flow}$$

$$\alpha_{\text{c}} = 2\,970.32\,\text{W·m}^{-2}\text{·K}^{-1}$$

The simple model mass fraction increase Δw along the absorber is 0.0696 kg·kg^{-1}. The vapour equilibrium line is linearized between $T_{\text{c},0}$ and T_{e} (dashed line in *figure 2*). With this choice the outcome for Δw is higher than for the simple model. A more obvious linearization, between T_0 and T_{e} (dash-dotted line in *figure 2*) results

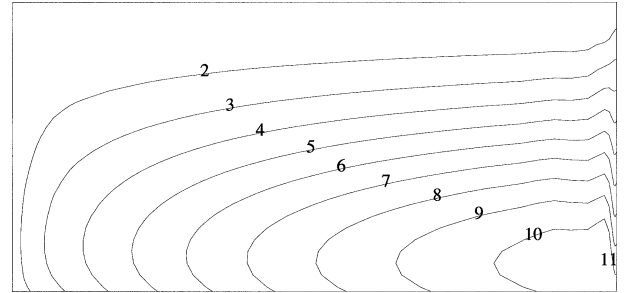
Figure 4. The flow lines in the gas phase. The Γ^{g} values in cm^2·s^{-1} for these lines are: 1: 0; 2: 3.53; 3: 7.06; 4: 10.59; 5: 14.12; 6: 17.64; 7: 21.17; 8: 24.70; 9: 28.23; 10: 31.76; 11: 35.29.

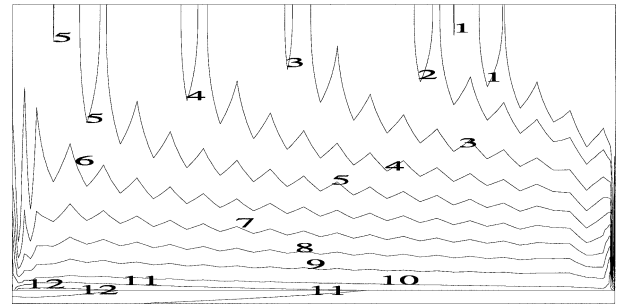**Figure 5.** The temperature contour lines in liquid and gas phase. Temperatures in °C: 1: −15; 2: −10; 3: 0; 4: 10; 5: 20; 6: 30; 7: 40; 8: 50; 9: 60; 10: 70; 11: 75; 12: 80.

in a Δw lower than the value for the simple model, but is rejected because it leads to w^{g} values larger than 1.

Figure 3 shows the velocity vector in the mesh points in the gas phase. The figure illustrates that the gas flow close to the interface is cocurrent, because of the no-slip condition (2a). *Figure 4* shows the flow lines. For the chosen width of the gas channel, the flow lines near the interface are almost identical for all three gas flow directions. *Figure 5* gives the isotherms, *figure 6* the mass fraction contour lines in liquid and gas phase. These lines show that convection dominates diffusion. Diffusion moves the curves a little bit towards $y = l_y$. Oscillations in the gas phase are a result of the applied element type (Section 2.3).
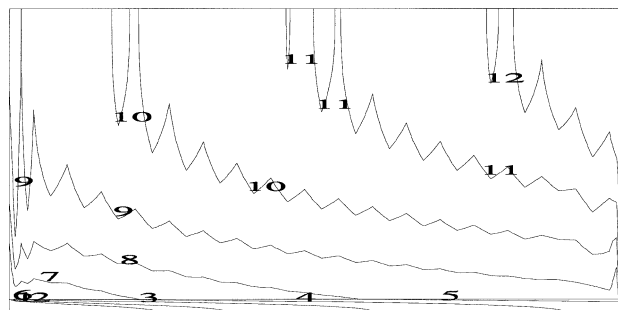
Figure 6. Mass fraction contour lines in liquid and gas phase. Ammonia mass fraction, in kg·kg^{-1}: 1: 0.08; 2: 0.09; 3: 0.11; 4: 0.13; 5: 0.15; 6: 0.7; 7: 0.75; 8: 0.8; 9: 0.85; 10: 0.9; 11: 0.95; 12: 0.99.
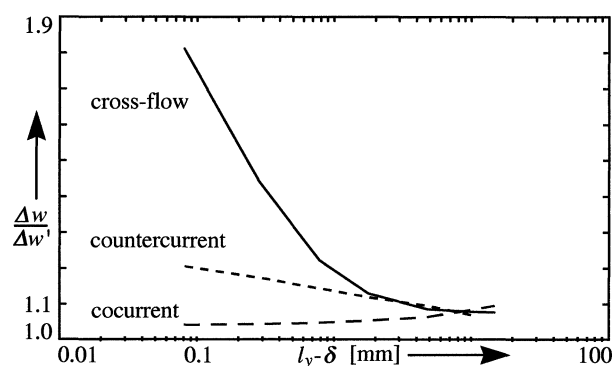

Figure 7. The ratio of the mass fraction increase Δw to the increase $\Delta w'$ from the simple model for several values of the effective gas channel width and three gas flow directions.

3.2. The effect of the gas channel width

Surprisingly, the effect of the direction of the gas flow on Δw over the absorber was small, less than 4 %! Also the deviation from the simple model outcome $\Delta w'$ is small, only 10 %. To find out the effect of the width of the gas channel, simulations were performed for other widths of the channel. *Figure 7* gives the results. For a channel smaller than 5 mm the differences between the outcomes for the three directions of gas flow increase for decreasing width. Cocurrent gas flow gives the lowest Δw value, because the interfacial gradients $\partial w/\partial y$ both decrease in flow direction. For countercurrent gas flow

more ammonia is absorbed, because the gas side gradient is large where the liquid side gradient is small. Cross-flow gives the best results, because here $\partial w^{\mathrm{g}}/\partial y$ is almost constant along the absorber.

For moderate and large channel dimensions the flow field in the immediate neighbourhood of the interface is not influenced any more by the entrance position of the vapour, and so is the absorption. More quantitatively: $D^{\mathrm{g}}l_x/(\Gamma l_y)$, the value of the ratio between diffusion and convection in the gas phase, determines the deviation of Δw from $\Delta w'$. For a significant effect, the ratio should exceed 1. For $l_y = 0.3$, 5 and 15 mm, respectively, the ratio is 19, 0.3 and 0.12 for mass transport and 15, 0.2 and 0.08, respectively, for heat transport. For small width (here 1 mm) assumption (3) is violated, because the drag force on the film becomes significant.

Acknowledgement

REFERENCES

[1] Grigor'eva N.I., Nakoryakov V.E., Exact solution of combined heat and mass transfer problem during film absorption, Inzhenerno-Fizicheskii Zhurnal 33 (1977) 893–898.

[2] Grossman G., Simultaneous heat and mass transfer in film absorption under laminar flow, Int. J. Heat Mass Transfer 26 (1983) 357–371.

[3] Wassenaar R.H., Simultaneous heat and mass transfer in a horizontal tube absorber; numerical tools for present and future absorbers, Thesis, TUD, 1994.

[4] Iedema P.D., Liem S.H., van der Wekken B., Heat and mass transfer in vapour and liquid phases of a H_2O/NH_3-regenerator, in: Proc. 15th Int. Congr. Refr. E2, Trondheim, 1985.

[5] Tsay Y.L., Lin T.F., Yan W.M., Cooling of a falling liquid film through interfacial heat and mass transfer, Int. J. Multiphase Flow 16 (5) (1990) 853–865.

[6] Wassenaar R.H., Simultaneous heat- and mass transfer in a one-dimensional film flow of a mixture with two components in the gas phase (final report), Report K-240 TUD, 1996.

[7] Segal A., Sepran Users Guide, Ingenieursbureau Sepra, Leidschendam, 1984.